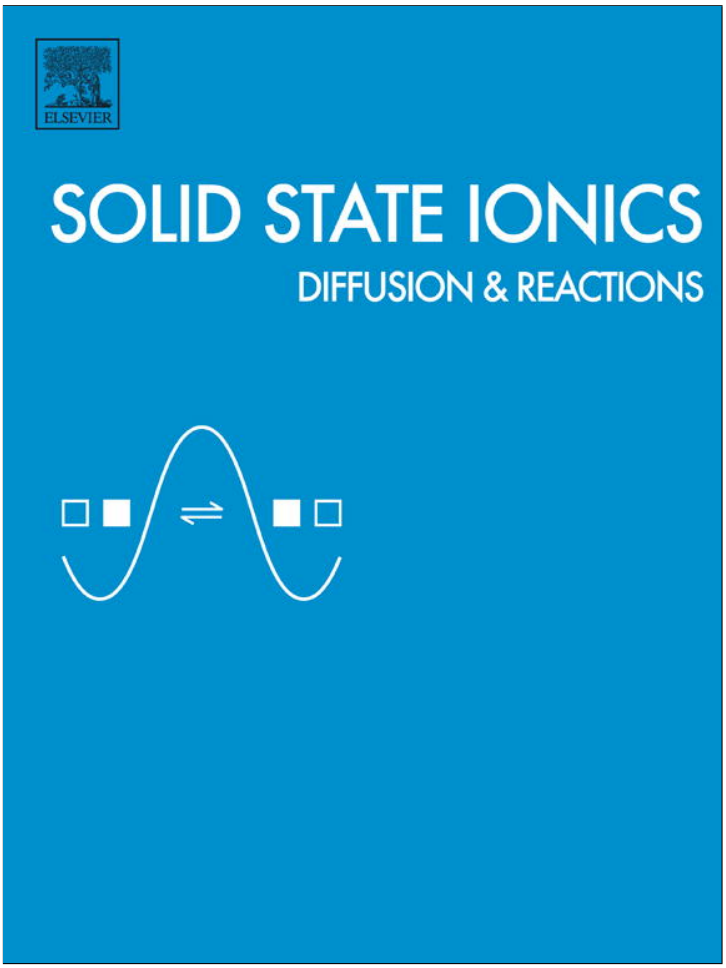

Solid State Ionics 240 (2013) 29–33

Contents lists available at SciVerse ScienceDirect

Solid State Ionics

journal homepage: www.elsevier.com/locate/ssi

Thermal behaviour of crystal and domain structure of LSGMn-05 anode material for SOFC

T. Tataryn [a,*], L. Vasylechko [b], D. Savytskii [c], M. Berkowski [d], C. Paulmann [e], U. Bismayer [f], A. Tarnavsky [g]

[a] State Scientific Research Control Institute of Veterinary Preparations and Fodder Additives, Donetska 11, 79019 Lviv, Ukraine
[b] Lviv Polytechnic National University, Bandera 12, 79013 Lviv, Ukraine
[c] Lehigh University, 5 East Packer Ave, Bethlehem, PA 18015, USA
[d] Institute of Physics Polish Academy of Sciences, Al. Lotników 32/46, 02-668 Warsaw, Poland
[e] HASYLAB, DESY, Notkestr. 85, D-22603 Hamburg, Germany
[f] Min.-Petrogr. Institute, Hamburg University, Grindelallee 48, D-20146 Hamburg, Germany
[g] Lviv State University of Life Safety, Kleparivska 35, 79000 Lviv, Ukraine

ARTICLE INFO

Article history:
Received 10 October 2012
Received in revised form 12 January 2013
Accepted 13 March 2013
Available online xxxx

Keywords:
Crystal structure
Twin structure
Phase transition
SOFC

ABSTRACT

The structure of perovskite-type $La_{0.95}Sr_{0.05}Ga_{0.95}Mn_{0.05}O_{3-x}$ crystals has been investigated using high-resolution X-ray powder diffraction technique in the temperature range of 298–1173 K. A transition from orthorhombic (*Pbnm*) to rhombohedral ($R\bar{3}c$) phase has been detected near 340 K. A chevron-like configuration of ferroelastic domain structure was observed in rhombohedral $La_{0.95}Sr_{0.05}Ga_{0.95}Mn_{0.05}O_{3-x}$ crystal using the Laue technique. The chevron-like pattern is formed by the intersection of *W*-type domain walls (211), (101) and (110) and demonstrates the reversibility of this domain wall structure configuration at thermal cycling through the phase transition point.

1. Introduction

Solid oxide fuel cells (SOFCs) are promising energy sources for appropriate applications [1–4]. The field of their possible application includes power installations, ranging from power supplies of portable electronic devices to power plants, which can operate in the range from 1 to 1000 kW [5–7]. In this time the industry is making two kinds of SOFCs – tubular and planar. Even though tubular SOFCs have progressed the most and are now nearing commercialization for stationary power generation, their power densities are low and manufacturing costs high. The low power density (0.25–0.30 W/cm^2) makes tubular SOFCs not very attractive for transportation and military applications. Planar SOFCs, in contrast, with very high power densities of up to about 2 W/cm^2, are ideally suited for these applications [5].

SOFCs have several features that make them more attractive than most other types of fuel cells [3,8]:

i) the highest efficiencies of all fuel cells, for combined heat and power applications increasing overall efficiencies to over 80%;
ii) the lifetime is more than 40000–80000 h;
iii) possibility of module construction and absent expensive metals like platinum;
iv) no problems with corrosion of components;
v) internal reforming of hydrocarbon fuels is possible.

Though solid oxide fuel cells have many physical and chemical advantages, the SOFCs technology still does not allow to develop inexpensive materials and production techniques. $LaGaO_3$ doped with Sr and Mn (LSGMn) is currently considered as a prospective anode material in SOFCs, especially for intermediate-temperature-SOFCs with $LaGaO_3$ doped with Sr and Mg (LSGM) as solid electrolyte [9,10]. LSGMn is chemically and physically compatible with LSGM electrolytes minimizing thus interfacial reactions, and have thermal expansion coefficients similar to that of LSGM.

Physical and chemical properties of crystalline materials are directly related to their global symmetry as well as to their microstructure. Ferroelastic domains and their twin boundaries are dominating features of the microstructure in LSGM. It was shown that diffusion of dopants or vacancies is fast along ferroelastic domain walls [11]. Furthermore, dopants can be concentrated in domain walls [12]. Recently, it was assumed [13,14], that high ionic conductivity of ferroelastic doped compounds with perovskite-type crystal structure ($LaGaO_3$) and, in particular, in compounds with nano-scale domains [15] is caused by additional oxygen migration along vacancies localized in domain walls. Keep in mind this we decide to devote present work to

* Corresponding author. Tel.: +380 322523152.
E-mail address: tataryn.taras@gmail.com (T. Tataryn).

0167-2738/$ – see front matter © 2013 Elsevier B.V. All rights reserved.
http://dx.doi.org/10.1016/j.ssi.2013.03.026

the structural investigations of $La_{0.95}Sr_{0.05}Ga_{0.95}Mn_{0.05}O_{3-x}$ (LSGMn-05) crystals in the temperature range of 298–1173 K and their twin structures in the ferroelastic phase.

2. Method of experiments

Single crystals of $La_{0.95}Sr_{0.05}Ga_{0.95}Mn_{0.05}O_{3-x}$ were grown by the Czochralski method in the Institute of Physics Polish Academy of Sciences (Warsaw, Poland) [9]. The evolution of the crystal structure in the temperature range of 298–1173 K has been studied by means of high-resolution X-ray powder diffraction using synchrotron radiation (beamline B2, HASYLAB, DESY). *In situ* high temperature powder diffraction experiments were performed using a STOE capillary furnace in Debye-Scherrer geometry and an on-site readable Image Plate detector OBI [16,17]. The powder was kept in 0.3 mm quartz capillaries. The wavelength of 0.65115 Å was calibrated using the reflection positions of Si (NIST SRM 640b) reference material. Crystallographic data were obtained by full profile Rietveld refinements technique using the WinCSD program package [18].

The ferroelastic domain structure of the LSGMn-05 crystal was determined using the Laue method. Samples with dimensions 0.2 × 0.2 × 0.2 mm^3 were selected using an optical microscope after grinding plates cut from a crystal boule. Samples were placed into a quartz capillary of 0.4 mm diameter and fixed using quartz wool. Corresponding experiments were carried out at beamline F1 at HASYLAB using a *Kappa*-diffractometer equipped with a MAR CCD detector. Dimensions of the CCD detector matrix were 16.5 × 16.5 cm with a resolution of 2048 × 2048 pixels. The available energy range of the synchrotron radiation was 5 to 60 keV. Laue patterns were collected at distances from specimen to detector of 100 and 300 mm in the temperature range from 293 to 973 K using a gas-flow heating device. Scanning of the specimen was carried out in the following angular ranges: $\varphi = 0° - 180°$ by 20°, $\chi = -90° - 0°$ by 15°, $\omega = 0°$, $\theta = 270°$. Laue patterns with the biggest splitting of reflections from orientation domains were selected for the analysis of the domain structure. An own program was used to determine the reflection coordinates on the Laue patterns. Indexing was performed using the OrientExpress V3.3 program [19].

3. Crystal structure

The analysis of the diffraction data lead to an orthorhombic *Pbnm* structure of LSGMn-05 at room temperature. *In situ* high-temperature X-ray synchrotron powder diffraction studies revealed a structural phase transition from an orthorhombic to rhombohedral $R\bar{3}c$ structure at about 340 K. The analysis of the diffraction patterns in the vicinities of the transition temperature revealed the coexistence of both, orthorhombic and rhombohedral phases, which gives evidence of the 1st-order character of the

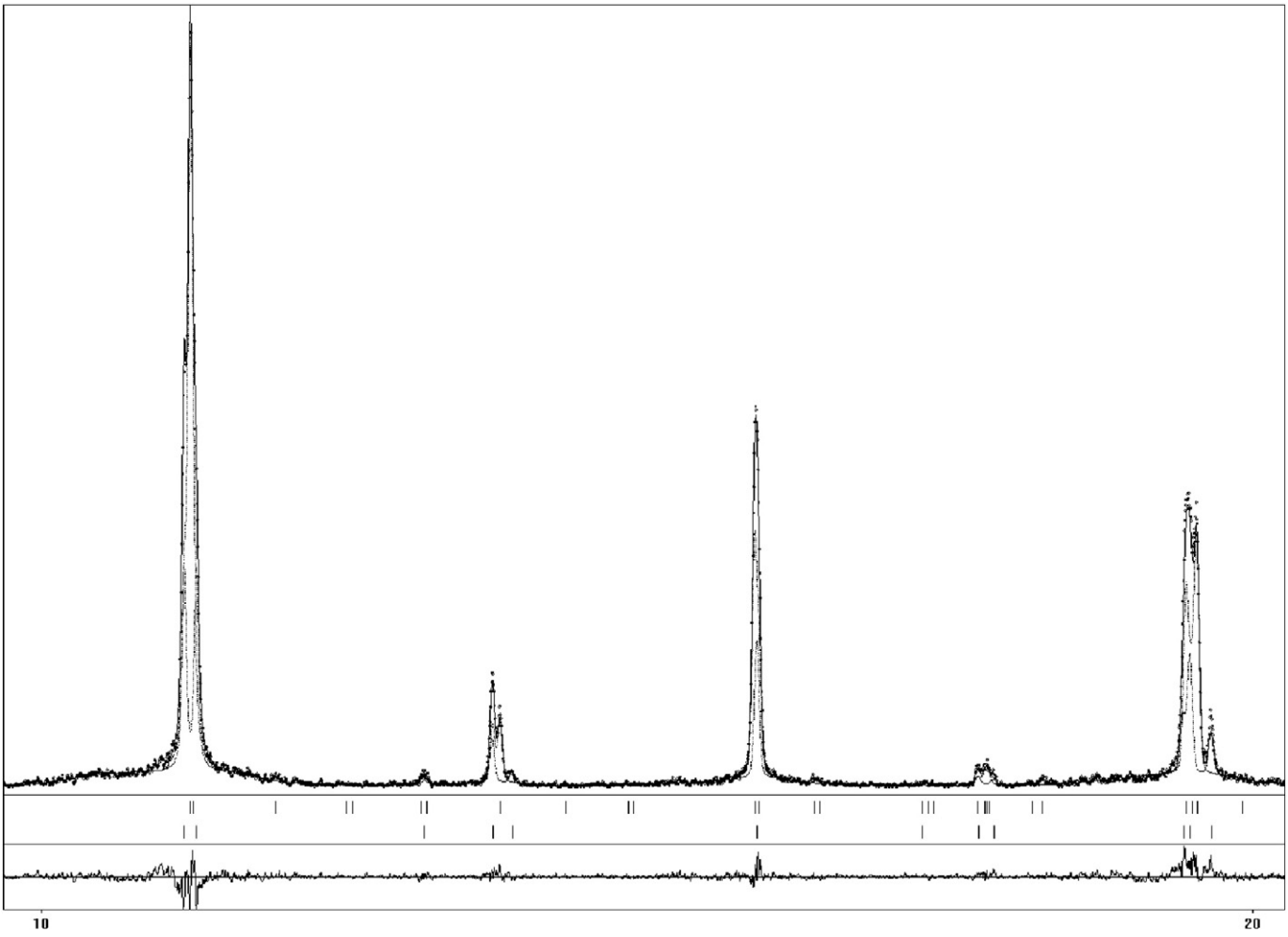

Fig. 1. Two-phase Rietveld refinement of LSGMn-05 with coexisting orthorhombic (66.2 wt.%) and rhombohedral (33.8 wt.%) phases at 338 K. Experimental (dots) and calculated patterns, as well as difference profiles are shown. The vertical bars indicate positions of diffraction maxima of orthorhombic and rhombohedral phases (upper and lower rows, respectively).

Table 1
Lattice parameters, positional and displacement parameters of atoms in different modifications of $La_{0.95}Sr_{0.05}Ga_{0.95}Mn_{0.05}O_{3-x}$.

Atoms, sites	Parameters	T = 303 K	T = 338 K		T = 1173 K
		Pbnm	*Pbnm* (76.2 wt.%)	$R\bar{3}c$ (23.8 wt.%)	$R\bar{3}c$
	a, Å	5.5246(2)	5.5266(2)	5.5259(3)	5.5668(2)
	b, Å	5.4883(2)	5.4896(2)	–	–
	c, Å	7.7707(3)	7.7724(3)	13.3567(7)	13.5411(6)
La(Sr),	*x*	−0.0036(5)	−0.0058(6)	0	0
6*a* in $R\bar{3}c$	*y*	0.0150(3)	0.0156(4)	0	0
4*c* in *Pbnm*	*z*	¼	¼	¼	¼
	B_{iso}, Å^2	0.79(3)	0.94(3)	0.93(7)	1.46(6)
Ga(Mn),	*x*	0	0	0	0
6*b* in $R\bar{3}c$	*y*	½	½	0	0
4*b* in *Pbnm*	*z*	0	0	0	0
	B_{iso}, Å^2	0.55(4)	0.93(5)	0.80(10)	1.13(10)
O1,	*x*	0.068(4)	0.078(5)	0.554(4)	0.555(4)
18*e* in $R\bar{3}c$	*y*	0.500(4)	0.508(5)	0	0
4*c* in *Pbnm*	*z*	¼	¼	¼	¼
	B_{iso}, Å^2	0.7(5)	1.4(7)	0.5(4)	1.7(5)
O2,	*x*	−0.273(4)	−0.278(5)	–	–
8*d* in *Pbnm*	*y*	0.271(4)	0.284(4)	–	–
	z	0.035(2)	0.030(3)	–	–
	B_{iso}, Å^2	0.5(3)	0.4(4)	–	–
R_I		0.0931	0.1230	0.2024	0.1230
R_P		0.1343	0.1450	0.1450	0.1636

phase transition. According to the results of a two-phase Rietveld refinement (Fig. 1, Table 1), the content of the orthorhombic phase decreases from 66.2 wt.% at 338 K to 26.5 wt.% at 343 K whereas the content of high temperature rhombohedral phase increases correspondingly.

Refined values of the structural parameters of orthorhombic and rhombohedral modifications of LSGMn-05 structure at room temperature, 338 and 1173 K are presented in Table 1.

Temperature evolution of the cell dimensions of both modifications of LSGMn-05 crystals, illustrating a discontinuous phase transition *Pbnm* — $R\bar{3}c$ is shown in Fig. 2.

From the extrapolation of the cell parameter ratio of the rhombohedral phase a continuous phase transitions from the rhombohedral to a cubic structure in the LSGMn-05 can be extrapolated to occur near 2063 K (Fig. 3).

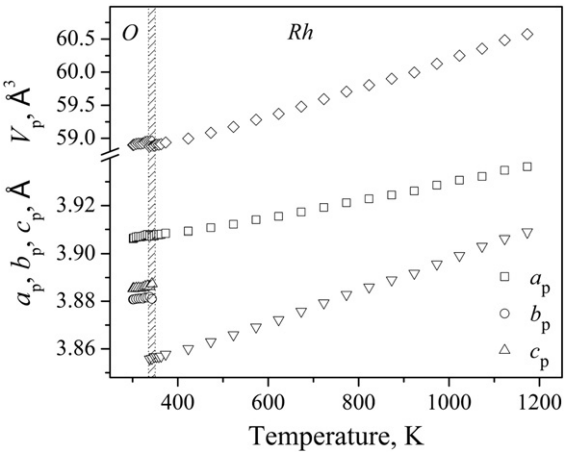

Fig. 2. Temperature dependences of lattice parameters and cell volumes of the orthorhombic (*O*) and rhombohedral (*Rh*) structure of LSGMn-05 in the temperature range 298–1173 K. Lattice parameters and cell volumes of the orthorhombic and rhombohedral cells are normalized to the perovskite ones as follows: $a_p = a_o/\sqrt{2}$, $b_p = b_o/\sqrt{2}$, $c_p = c_o/2$, $V_p = V_o/4$; $a_p = a_r/\sqrt{2}$, $c_p = c_r/\sqrt{12}$, $V_p = V_r/6$.

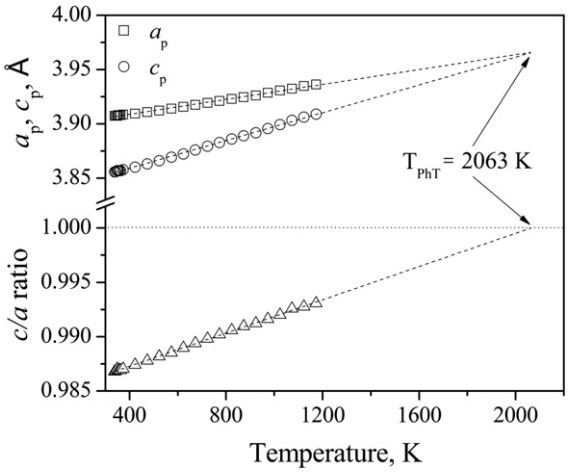

Fig. 3. Lattice parameters and their ratio of rhombohedral LSGMn-05 in the temperature range 338–1173 K and extrapolation to an expected phase transition of cubic symmetry.

4. Domain structure

Analysis of the Laue patterns showed that the LSGMn-05 crystal has a twin configuration of four domains in the high temperature rhombohedral phase as shown in the Laue pattern (Fig. 4), which was obtained at 380 K and a CCD-sample distance of 100 mm. The symbols *D1*, *D2*, *D3* and *D4* indicate different ferroelastic orientation states and the corresponding reflections. This corresponds to the results of the theoretical analysis of the ferroelastic domain structure in rhombohedral $La_{0.95}Sr_{0.05}Ga_{0.9}Mg_{0.1}O_{3-x}$ (LSGM-05) [20] and we can expect the appearance of domain walls with orientation {110} and {211}.

The identification of domain walls in the rhombohedral LSGMn-05 crystal was performed using the "relative displacement" algorithm [21,22]. The algorithm consists of:

1) determination of coordinates of reflections from one orientation state;
2) indexing and determination of the orientation matrix, which specifies the orientation of the basis vectors of the unit cell of the domain relative to the coordinate system;
3) determination of connecting matrices between the domains;
4) determination of orientation matrices of adjacent domains;

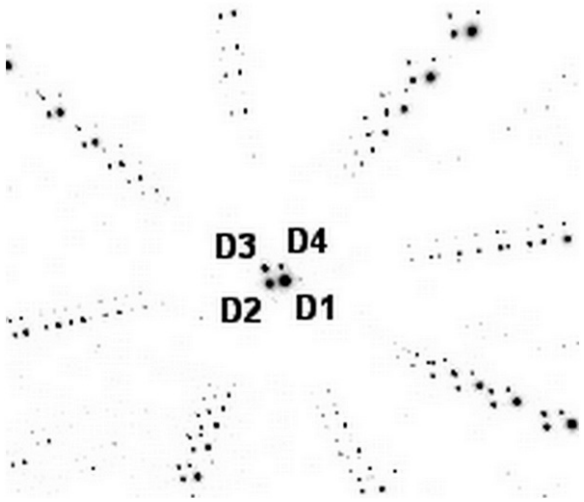

Fig. 4. Section of a Laue diffraction pattern of a LSGMn-05 crystal detected at 380 K at a CCD-sample distance of 100 mm.

5) simulation of a theoretical Laue pattern using orientation matrices of all possible domains and comparison with its experimental Laue pattern.

It was found that the domains are interconnected by twin walls – i.e. mirror planes with Miller indexes (211), (101) and (110) (Fig. 5). Due to the intersection of those walls a chevron-like domain pattern was formed, which results from the relaxation of the structural strain caused by the cubic → rhombohedral phase transition.

5. Temperature behaviour of twin structure

The reversibility of the characteristic chevron-like domain structures during the transformation between ferroelastic phases of LSGM-05 crystal was described in [23]. The discovered reversibility of domain structure in this perovskite crystal follows from the memory of microstrain caused by space distribution of oxygen vacancies and dopant ions in the crystal. In another electrolyte material with the fluorite structure – ZrO_2 crystal doped with 10 mol % Sc_2O_3 – no reversibility of the domain structure during temperature cycling to the paraelastic cubic phase was observed [22]. The non-reversibility of the domain structure is probably caused by dominating strains resulting from a mismatch of the phases during the ferroelastic phase transformation. Taking into account the segregation of oxygen vacancies into domain walls, it has been proposed that the high ionic conductivity of LSGM-05 compounds is caused by two simultaneous processes of oxygen diffusion: through the bulk of the domains and along domain boundaries [13]. In doped ZrO_2 the interaction of domain boundaries with oxygen vacancies is not dominant, so additional diffusion of oxygen along domain walls gives a smaller contribution to the ionic conductivity of ZrO_2:Sc_2O_3 solid solutions. This can cause smaller ionic conductivity of those compounds as compared to solid solutions based on lanthanum gallate.

To investigate the interaction of oxygen vacancies and the domain boundaries in LSGMn-05, we measured the evolution of the domain structure during thermal cycling through the phase transition point. Experiments were carried out at beamline F1 in the range from 300 to 380 K. Laue patterns collected after series of thermal treatments of samples above the ferroelastic phase transition have been analyzed.

Since the crystal was heated above the ferroelastic phase transition temperature the twin structures of the low temperature orthorhombic phase (Fig. 6, a) are re-arranged into other twin structures, characteristic for the rhombohedral phase (Fig. 7, a). Upon cooling to room temperature the twin walls rearrange again (Fig. 6, b). Analysis of the intensities of the multiplets in the Laue diffraction patterns of LSGMn-05 crystal showed that the twin configurations emerging during the temperature cycling between orthorhombic and rhombohedral ferroelastic phases can be described as follows: Z → X → Y → X → Y → …, where Z is the initial twin configuration in the

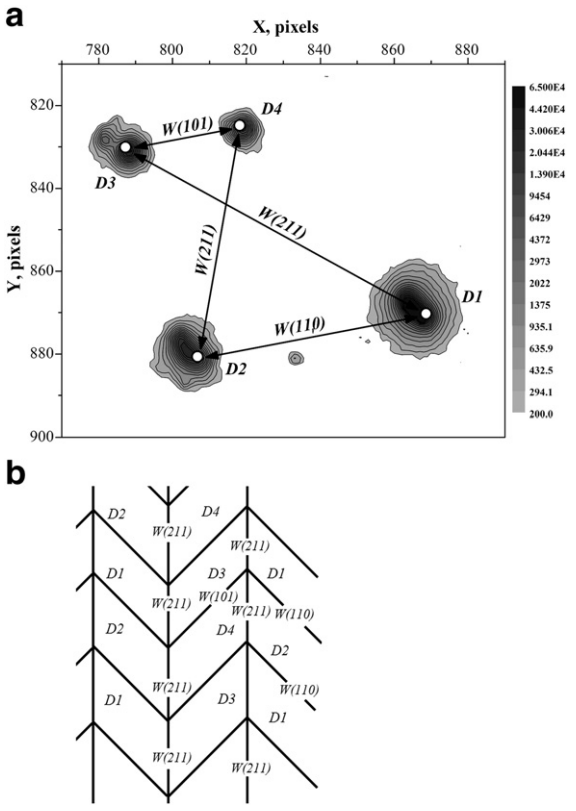

Fig. 5. Section of Laue pattern collected at a CCD-sample distance of 300 mm with calculated spot positions for twin walls of LSGM-05 (with respect to domains *D3*) (a) and model of the chevron-like twin structure in the rhombohedral phase formed by *W*-type domain walls (211), (101) and (110) (b).

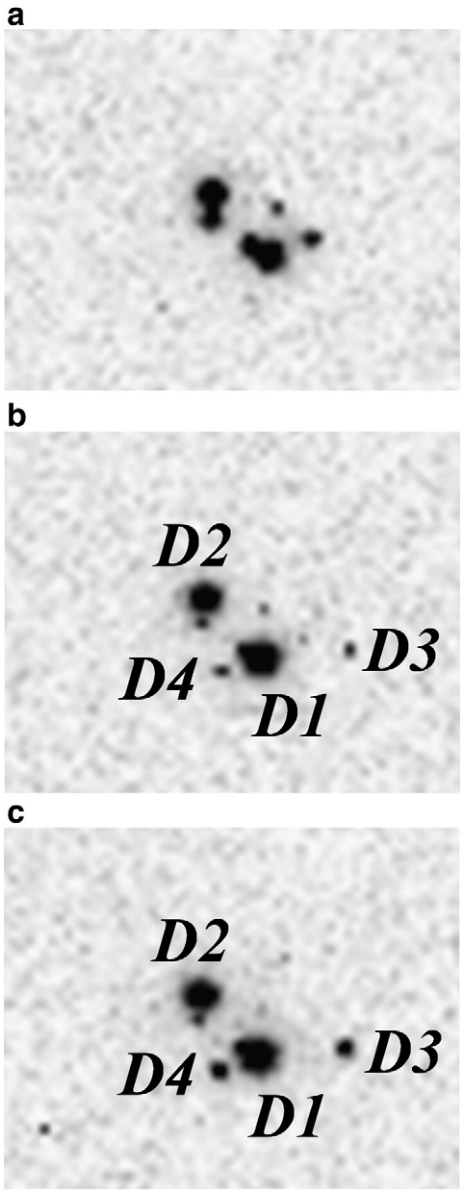

Fig. 6. Three sections of Laue patterns collected at 300 K before first (a), after first (b) and second (c) heating of LSGMn-05 specimen above temperature of ferroelastic phase transition to rhombohedral phase.

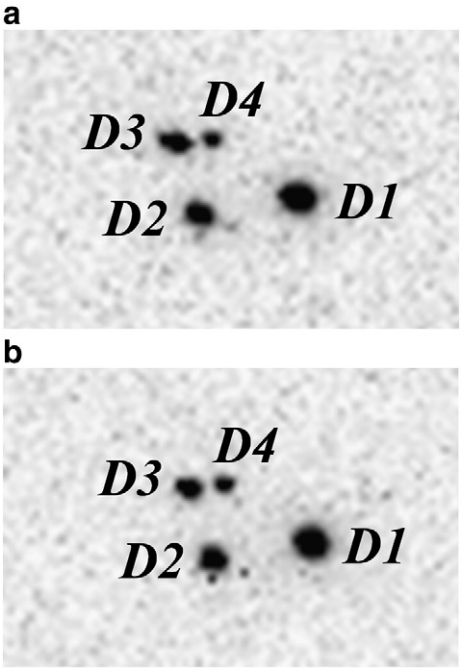

Fig. 7. Two sections of Laue patterns collected at 380 K during first (a) and second (b) heating of LSGMn-05 specimen.

orthorhombic phase prior to the first heating; X is the twin configuration formed in the rhombohedral phase after heating; Y is the twin configuration emerging in the orthorhombic phase (instead of the initial one) after cooling below the rhombohedral transition point. Thus, after the first thermal cycle the crystals "switch" between two phase-specific twin configurations (Fig. 6, 7), which are fully reproduced in both ferroelastic phases. But the volumes of each orientation state are not fully reproduced in both ferroelastic phases (Table 2). Table 2 shows the ratio of intensities of reflections from each of the other three orientation states to the intensity of the *D1* state in the LSGMn-05 crystal. After repeated temperature cycles the ratios of intensities are not completely identical. This may be caused by incomplete relaxation of strain, which may arise during the sample preparation, because the LSGMn-05 crystal was heated only up to 380 K.

Only the twin structure observed in the orthorhombic phase prior to the first phase transition is an exception. In order to understand this it should be taken into account that the sample was prepared through mechanical fragmentation at room temperature, which causes additional strain in the crystal. The corresponding twin structure is a "non-equilibrium" state because both, the crystal shape and its size changed after the sample preparation. The "equilibrium" twin structure is formed in the rhombohedral phase on heating above the transition point.

Evidently, a domain wall location memory of domain structure in LSGMn-05 is caused by dominating mechanical strains caused by the distribution of point defects in the crystals at the phase transformation from the rhombohedral ferroelastic to orthorhombic ferroelastic phase, such as in LSGM-05.

Table 2
The ratio of reflection intensities from orientation states related to the intensity of the *D1* state.

Ratio of intensities	In orthorhombic phase, after 1st temperature cycling	In orthorhombic phase, after 2nd temperature cycling	In rhombohedral phase, during 1st temperature cycling	In rhombohedral phase, during 2nd temperature cycling
I_{D2}/I_{D1}	0.99	0.96	0.28	0.19
I_{D3}/I_{D1}	0.01	0.10	0.70	0.56
I_{D4}/I_{D1}	0.01	0.03	0.39	0.26

6. Conclusions

In situ powder diffraction studies showed that the orthorhombic *Pbnm* phase of $La_{0.95}Sr_{0.05}Ga_{0.95}Mn_{0.05}O_{3-x}$ transforms into a rhombohedral phase with space group $R\bar{3}c$ at about 340 K. Coexistence of the low and high temperature phases at the transition temperature indicates a discontinuous character of the phase transition.

Twinning of the perovskite-type crystals $La_{0.95}Sr_{0.05}Ga_{0.95}Mn_{0.05}O_{3-x}$ was studied using the Laue method. In the rhombohedral phase of the crystal, four domains separated by *W*-type twin walls (211), (101) and (110) occur. The intersection of these walls leads to the formation of a chevron-like pattern and allows for a stress-free co-existence of the four orientation states.

The reversibility of the domain structure during the temperature cycling observed in the $La_{0.95}Sr_{0.05}Ga_{0.95}Mn_{0.05}O_{3-x}$, is probably caused by the memory of microstrains, which result from the spatial distribution of point defects in the crystal.

Acknowledgment

The work was supported in parts by WTZ (UKR 07/009), the Ukrainian Ministry of Education and Science (projects "Tern" and "Neos") and ICDD Grant-in-Aid program.

References

[1] A.B. Stambouli, E. Traversa, Renewable Sustainable Energy Rev. 6 (2002) 433–455.
[2] B.C.H. Steele, A. Heinzel, Nature 414 (2001) 345–352.
[3] S. Haile, Mater. Today 6 (2003) 24–29.
[4] N.Q. Minh, J. Am. Ceram. Soc. 76 (1993) 563–588.
[5] S.C. Singhal, Solid State Ionics 152–153 (2002) 405–410.
[6] A. Weber, E. Ivers-Tiffée, J. Power Sources 127 (2004) 273–283.
[7] D. Stöver, H.P. Buchkremer, S. Uhlenbruck, Ceram. Int. 30 (2004) 1107–1113.
[8] H. Tu, U. Stimming, J. Power Sources 127 (2004) 284–293.
[9] M. Glowacki, T. Runka, V. Domukhovski, R. Diduszko, M. Mirkowska, M. Berkowski, B. Dabrowski, J. Alloys Compd. 509 (2011) 1756–1759.
[10] Q. Fu, X. Xu, D. Peng, X. Liu, G. Meng, J. Mater. Sci. 38 (2003) 2901–2906.
[11] A. Aird, M.C. Domeneghetti, F. Mazzi, V. Tazzoli, E.K.H. Salje, J. Phys. Condens. Matter 10 (1998) 569–574.
[12] M. Bartels, V. Hagen, M. Burianek, M. Getzlaff, U. Bismayer, R. Wiesendanger, J. Phys. Condens. Matter 15 (2003) 957–962.
[13] M. Kurumada, E. Iguchi, D. Savytskii, J. Appl. Phys. 100 (2006) 014107.
[14] E. Iguchi, D. Savytskii, M. Kurumada, in: Ja.Y. Murdoch (Ed.), Diffusion and Reactivity of Solids, Nova Science Publishers, Inc., New York, 2007.
[15] A. Skowron, P. Huang, A. Petric, J. Solid State Chem. 143 (1999) 202–209.
[16] M. Knapp, V. Joco, C. Baehtz, H.H. Brecht, A. Berghaeuser, H. Ehrenberg, H. von Seggern, H. Fuess, Nucl. Instrum. Methods A 521 (2004) 565–570.
[17] C. Baehtz, H. Ehrenberg, H. Fuess, J. Synchrotron Radiat. 11 (2004) 328–334.
[18] L.G. Akselrud, P.Yu. Zavalij, Yu. Grin, V.K. Pecharsky, B. Baumgartner, E. Wölfel, Mater. Sci. Forum 133–136 (1993) 335–342.
[19] www.ccp14.ac.uk/ccp/web-mirrors/lmgp-laugier-bochu/.
[20] D. Savytskii, U. Bismayer, Phase Transitions 81 (2008) 431–447.
[21] T. Tataryn, D. Savytskii, L. Vasylechko, C. Paulmann, U. Bismayer, H. Boysen, Phys. Status Solidi C 6 (2009) 1178–1181.
[22] T. Tataryn, D. Savytskii, C. Paulmann, U. Bismayer, Radiat. Phys. Chem. 78 (2009) S101–S104.
[23] D.I. Savytskii, L. Vasylechko, U. Bismayer, C. Paulmann, M. Berkowski, NATO Sci. Ser. 202 (2005) 135–148.